



ARCHIVES  
of  
FOUNDRY ENGINEERING

ISSN (2299-2944)  
Volume 2022  
Issue 3/2022

53 – 59



10.24425/afe.2022.140236

7/3

Published quarterly as the organ of the Foundry Commission of the Polish Academy of Sciences

# Influence of Melt Quality on the Formation of Fe Intermetallic in A360 Alloy

E.N. Bas<sup>a</sup>, S. Alper<sup>a</sup>, T. Tuncay<sup>b</sup> , D. Dispinar<sup>c</sup> , S. Kirtay<sup>a</sup> 

<sup>a</sup> Istanbul University-Cerrahpasa, Turkey

<sup>b</sup> Karabuk University, Turkey

<sup>c</sup> Foseco, Netherlands

Received 14.04.2022; accepted in revised form 01.06.2022; available online 07.09.2022

## Abstract

The solubility of Fe in aluminium alloys is known to be a problem in the casting of aluminium alloys. Due to the formation of various intermetallic phases, the mechanical properties decrease. Therefore, it is important to determine the formation mechanisms of such intermetallic. In this work, A360 alloy was used, and Fe additions were made. The alloy was cast into the sand and die moulds that consisted of three different thicknesses. In this way, the effect of the cooling rate was investigated. The holding time was selected to be 5 hours and every hour, a sample was collected from the melt for microstructural analysis. Additionally, the melt quality change was also examined by means of using a reduced pressure test where the bifilm index was measured. It was found that the iron content was increased after 2 hours of holding and the melt quality was decreased. There was a correlation between the duration and bifilm index. The size of Al-Si-Mn-Fe phases was increased in parallel with the bifilm content regardless of the iron content.

**Keywords:** A360, Fe intermetallic, Melt quality, Cooling rate

## 1. Introduction

The use of secondary aluminium alloy is economical compared to primary aluminium. Rejected parts, runners, and feeders can be used as the source material. Scrap can be collected and used as an aluminium source. In such applications, several additional operations are required like degassing with an aim to achieve and start with a clean melt. However, one critical parameter is obtaining the proper chemical composition of the alloy within the given standard ranges. A typical problem faced in aluminium recycling is the high Fe content. In many die casting applications, aluminium quickly reacts with the mould and can therefore dissolve iron. The solubility of Fe leads to the formation of various complex intermetallic phases which are known to be harmful to the mechanical properties [1-5]. Actually, in some high pressure die casting operations, iron is deliberately added to melt to prevent the mould/metal reaction which is also known as

sticking. On the other hand, the way to remove the increased iron content in the liquid metal is not economically feasible. Therefore, many works have been carried out to characterise the formation of different iron phases. Due to their stability, they have high physical, thermal, and mechanical resistance. Due to their high hardness, low material density compared to iron, high resistance to corrosion and oxidation, they are sometimes preferred. These intermetallic have high melting temperatures almost twice the melting temperature of aluminium. Therefore, the intermetallic in molten aluminium continues to exist in the liquid metal. Ductility and fracture toughness values decrease at room temperature after casting of parts containing these intermetallic because these phases are brittle. The presence of Mn and Cr together with Fe and Si in the structure can nucleate various phases [6-8]. These Fe - rich primary phases are called sludge. During the holding time of the liquid metal, the sludge phase tends to sediment to the bottom of the crucible. Therefore, the formation of sludge changes the chemical composition of the



liquid metal. In addition, these particles reduce the viscosity of the alloy. Due to their hardness, they can erode the mould surfaces, shorten the tool life and damage the used machines mechanically and physically during their long service life. Additionally, the effect of the cooling rate has been studied where the change in morphology of these phases was investigated [9-11]. Fe phases were also associated with porosity [12-14]. Cao [15-18] proposed that Fe phases were nucleating on bifilms and this was the reason for porosity, lowered fluidity, and mechanical properties. Bjurenstedt [19] used microfocus X-ray to in-situ observe the nucleation and growth of Fe intermetallics in A380 alloy. It was reported that the oxide surfaces of the samples are strongly suggested to be a nucleation site for the Fe-rich intermetallics and at higher cooling rates, star-shaped phases were observed. Shabestari [20] reported that with increased Mn and Fe, the size and the number of star-like intermetallics were increased. Ferraro [21] found similar findings where the effect of Cr was also included.

In this work, the formation of Fe-intermetallic with regard to the melt quality was investigated. The cleanliness of the melt is defined by the presence of oxides called bifilms. These bifilms can act as heterogeneous nucleation sites for intermetallic. Their quantity can be determined quantitatively by a reduced pressure test.

## 2. Experimental work

In this work, A360 alloy with the chemical composition given in Table 1 was used. Pure iron swarf was pressed in the form of cylindrical pellets (Figure 1).

Table 1.

Chemical composition of A360 alloy (wt%)

| Si  | Fe  | Cu   | Mn   | Cr    | Mg  | Zn   | Ti   | Al   |
|-----|-----|------|------|-------|-----|------|------|------|
| 9,1 | 0,3 | 0,07 | 0,45 | 0,002 | 0,5 | 0,01 | 0,06 | Rem. |



Fig. 1. Pure iron pellets used in the tests

They were dipped into the melt at 750°C in a 1 kg crucible melted in a resistance furnace. Five crucibles were prepared, and the alloy was kept at the temperature for 5 hours. Every hour, one of the crucibles was used to cast permanent (1040 steel) and sand mould samples where the dimension is given in Figure 2 with the aim to simulate the effect of cooling rate on the microstructure. Investigations, microstructural and Fe-phase analysis were conducted from the centre of each step in the mould (Fig 2c).

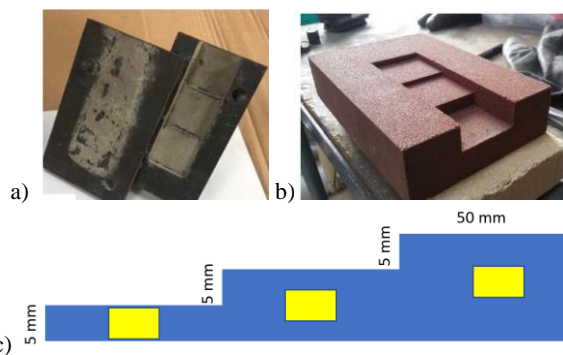


Fig. 2. Moulds used in the tests (a) permanent, (b) sand mould, (c) dimension of the part and analysis locations marked in yellow

A reduced Pressure Test (RPT) was used to solidify 180 g of a sample under 100 mbar. To quantify the melt cleanliness, bifilm index [22] was measured from the cross-section of RPT samples. FoundryMaster Spectral analysis was used to measure the alloy content of the melts. JEOL 5600 SEM (Scanning Electron Microscope) was for the phase analysis. The sludge factor was measured based on the following equation [2], [21]:

$$\text{Sludge Factor} = (1 \text{ wt\% Fe}) + (2 \text{ wt\% Mn}) + (3 \text{ wt\% Cr})$$

## 3. Results

The change in the porosity number and size in the cross-section of RPT samples at different holding of Fe in the melt is given in Figure 3. It is interesting to note that the number of pores was decreasing significantly while their sizes increased dramatically. The decrease in the number of pores is possibly due to the sedimentation of Fe phases on bifilms as was suggested by Gyarmati [23]. Similar RPT samples and pore distributions were observed in their study.

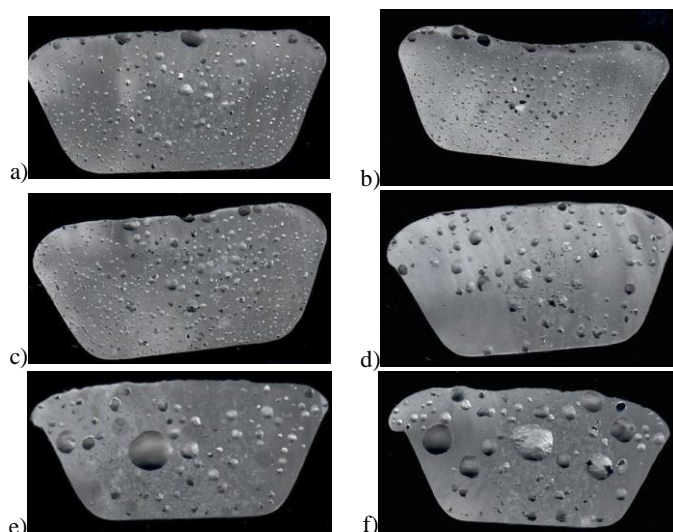


Fig. 3. RPT sample cross-sections of (a) 0, (b) 1, (c) 2, (d) 3, (e) 4 and (f) 5 hours of holding time

The change in the Fe content and sludge factor with the bifilm index of the melt with the duration of the liquid A360 alloy is given in Figure 4. As can be seen in Figure 4a, the Fe content is increasing in the melt in 1<sup>st</sup> and 2<sup>nd</sup> hour but decreases after 4 hours and tends to increase once again after 5 hours whereas bifilm index is increasing almost linearly after 5 hours for every hour. On the other hand, the sludge factor remained almost unchanged between 1-1.2 as seen in Figure 4b which is quite low [21].

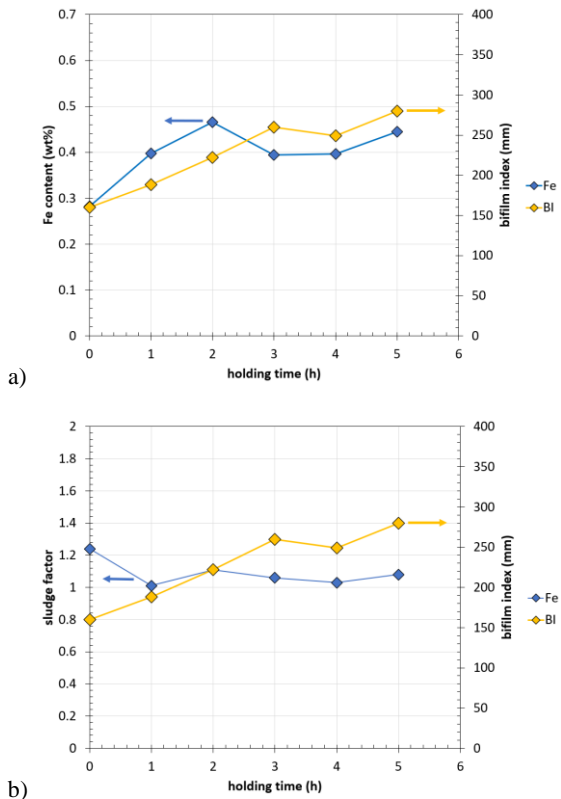


Fig. 4. Change in (a) Fe content and (b) sludge factor with bifilm index with holding time

Contour maps were plotted between duration, bifilm index, Fe content, and sludge factor. The results are summarised in Figure 5. It can be seen that as the duration was increased, both Fe content and bifilm index were increased (Fig 5a) whereas sludge factor was decreased with increased duration and increased bifilm index (Fig 5b).

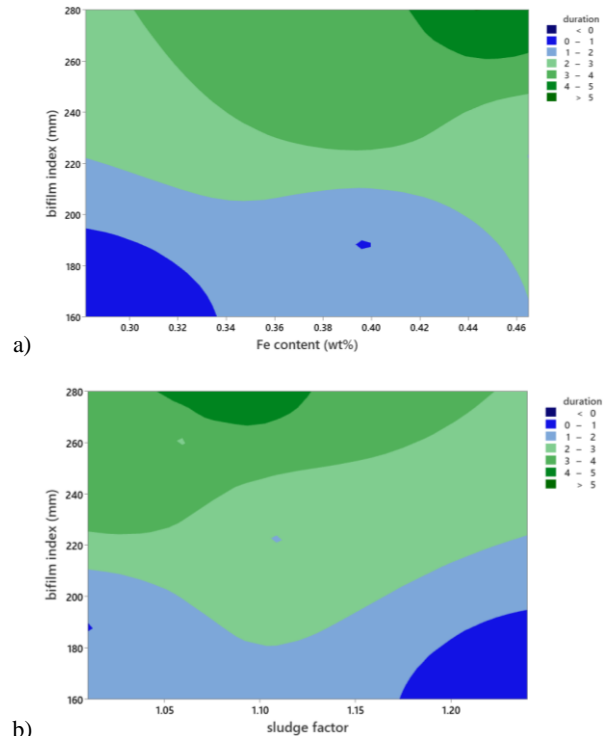


Fig. 5. Contour map of duration, bifilm index, and (a) Fe content and (b) sludge factor

The main effects plot for the bifilm index with regard to Fe content and duration is given in Figure 6. It can be seen that duration has a more significant effect on the bifilm index than Fe content.

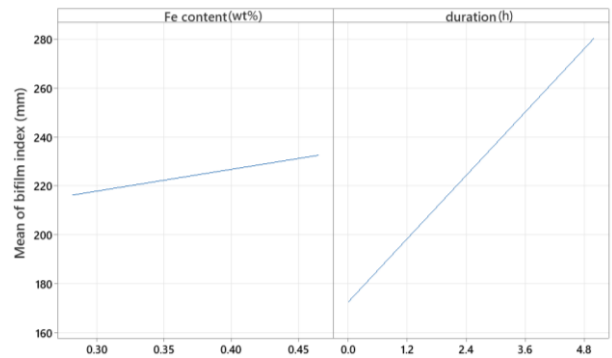


Fig. 6. Main effects plot of bifilm index

In Figure 7, SEM images and EDX analysis of Fe intermetallic formed for the duration of holding times on which the samples were cast in a sand mould. Up until 2 hours of holding, the content of Fe intermetallic is quite low which is in good agreement with Fe content and sludge factor. Almost all of the phases are predominantly in the form of Chinese-script (skeleton) morphology. A similar scenario applies to microstructures of samples cast in the permanent mould. As seen in SEM images in Figure 8, the morphology of Fe intermetallic is script-like a-phase

however due to faster cooling rate in die mould, their size and thicknesses are smaller.

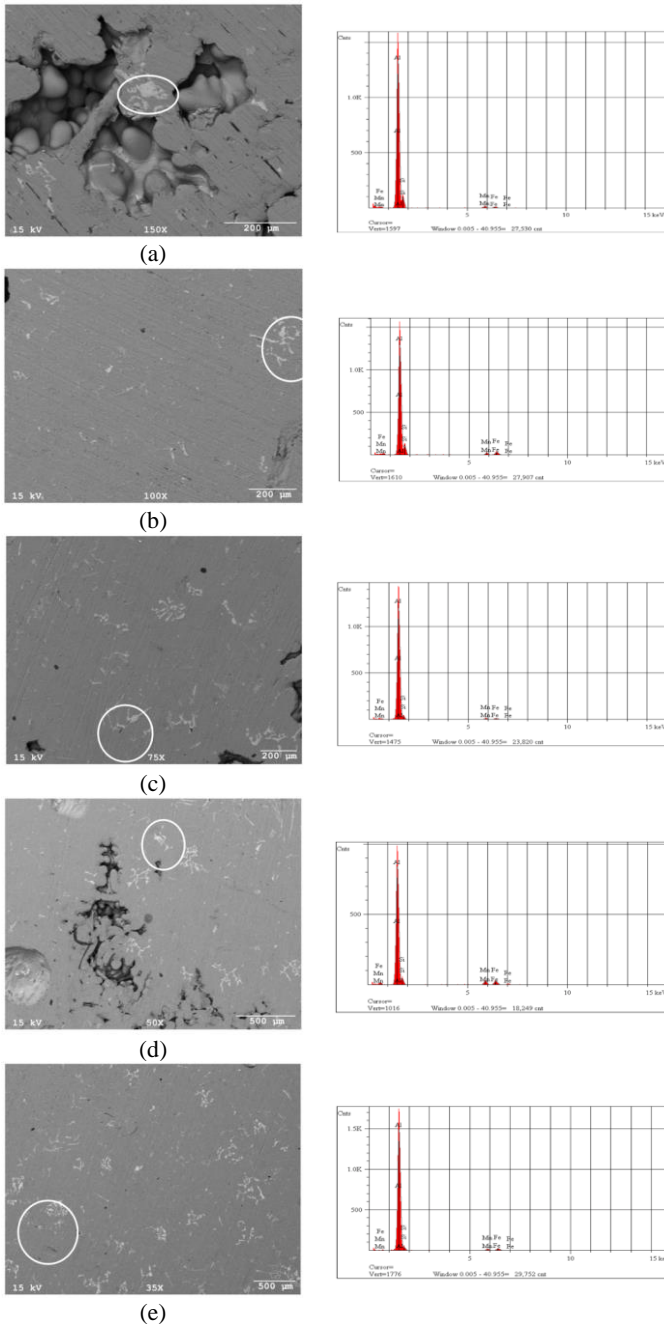


Fig. 7. SEM images of samples cast in sand mould held for (a) 1, (b) 2, (c) 3, (d) 4 and (e) 5 hours

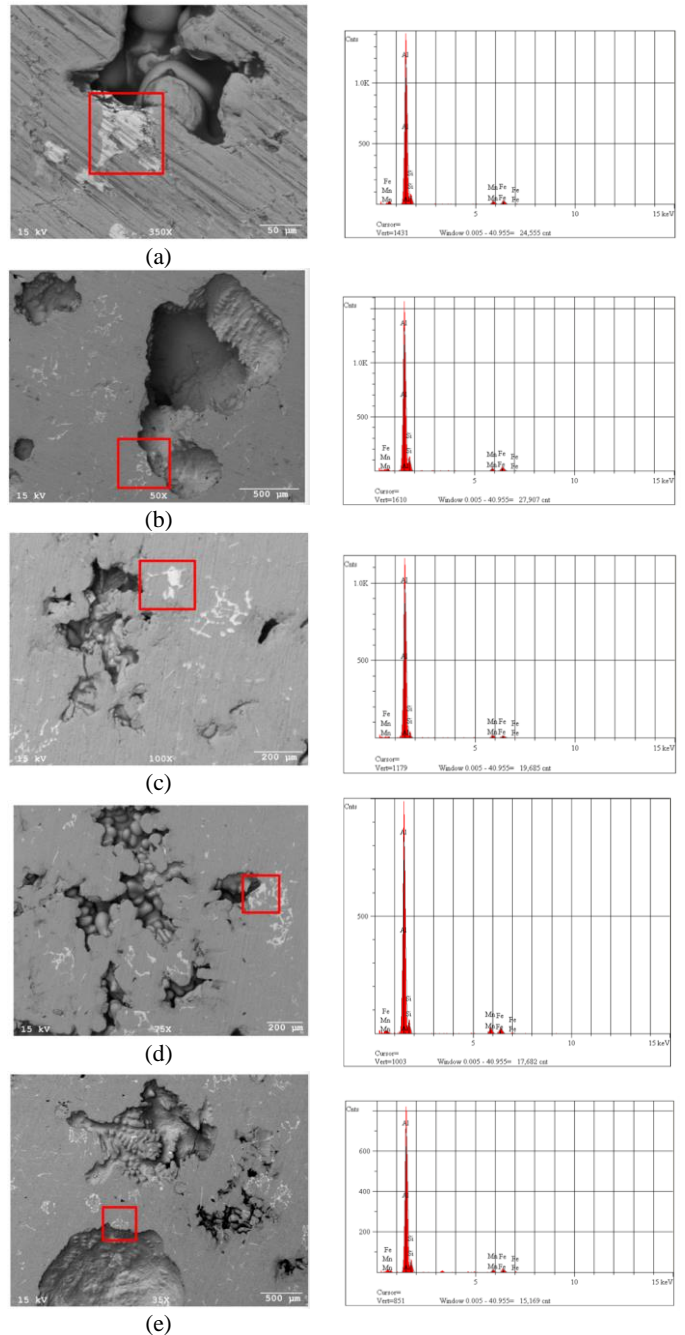


Fig. 8. SEM images and EDS analysis of samples cast in permanent mould held for (a) 1, (b) 2, (c) 3, (d) 4, and (e) 5 hours

The length of the Al-Si-Fe-Mn phases was measured, and the results can be seen in Figure 9. It can be seen that the average length is around 180 μm in both of the castings: sand and permanent. It is interesting to note that the size of Fe-phases was not affected by the section thickness and mould type studied in this work. However, the scatter in the permanent mould appears to be higher compared to the sand mould. Ferrara [21] had observed a scatter of 50 μm difference in their work.

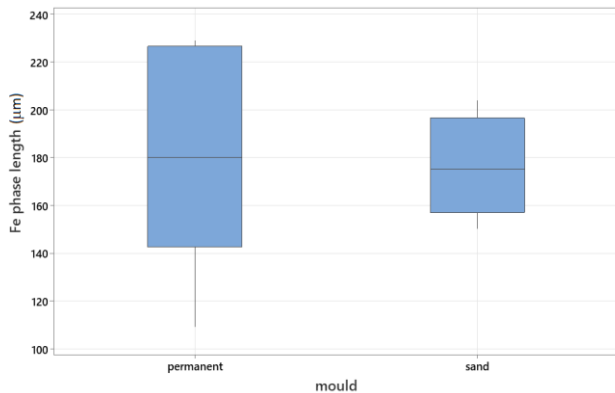


Fig. 9. The average length of Fe phases

The change in the Al-Si-Fe-Mn phase length with bifilm index, Fe content, and mould type are given in Figure 10. The most significant observation in this graph is the increase in Fe phase length by bifilm index, whereas there was no direct correlation with the mould type or iron content. This finding is confirmed by the Pareto chart given in Figure 11. It can be seen that the effect of bifilm index on Fe phase length is around 2 whereas other parameters such as mould type, Fe content, and duration are around 0.5 factorial.

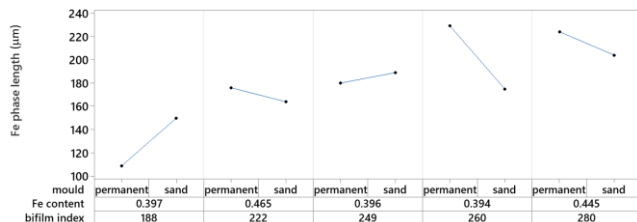


Fig. 10. Average Al-Si-Fe-Mn phase length with bifilm index, Fe content, and mould type

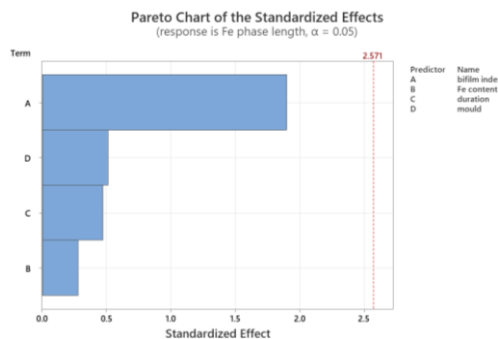


Fig. 11. Pareto chart of Al-Si-Fe-Mn phase length with bifilm index, Fe content, duration, and mould type

## 4. Discussion

The behaviour of Al-Si-Fe-Mn intermetallic in aluminium alloys affects the liquid metal quality and the mechanical properties of the material. The dissolution and diffusion of iron in

liquid metal have been the subject of many studies. In this work, it was found that there is an increase in iron diffusion to liquid metal over time. However, this increase in Fe content was not so linear. One of the main reasons for this is the use of Fe pellets. In an unpublished work of the authors, the iron rod was dipped into the melt and the Fe content was found to increase linearly by duration. When pellets were used (which were produced from the swarf that was pressed), the surface tension and wettability of the Fe pellet with the liquid aluminium appear to play a significant role in the diffusion of the Fe into the melt. The alloy used was 360, and it contained Mn and Cr, therefore the phases found in the microstructure were a-Fe intermetallic in the form of the skeleton but mostly Chinese script rarely needle-like morphology. In the step mould, the thickness of each step varies inversely with the cooling rates. Intermetallic formation decreases slowly when the cooling occurs fast because the amount of intermetallic in the unit area decreases and it does not find the time to nucleate. Considering that the amount of iron diffusing into the structure increases with time and that there is a potential amount of iron for the intermetallic phase formation, it is observed that the cause of the increase in the average length of the Al-Si-Fe-Mn phases was related to bifilm index. As the bifilm index was increased (Figure 10-11), the average length of Fe phases was increased. The number of porosities decreased as the waiting time increased, but the sizes increased. Iron content also increases with holding time, but diffusion is limited after a certain time. This is because the intermetallic formed during solidification were nucleated on bifilms.

Podprocká [24] added different ratios of Mn to A356 alloy from 0.1 to 0.7 wt%. The average length of  $\alpha$ -Fe phases was found to be changing between 20-75 mm in die cast samples. Liu [10] showed that at a high cooling rate,  $\beta$ -Fe formation is observed in sizes ranging from 200-230 mm. Samuel [25] found that beta size was between 145-167 mm. Ma [3] claimed that  $\beta$ -Fe size above 70 and 100 mm deteriorates the tensile properties in direct chill cast 3xx alloys. The variability chart in Figure 10 shows that the average length of Al-Si-Fe-Mn phase was dominantly affected by the increase in the bifilm index rather than the Fe content and cooling rate (i.e. sand and permanent moulds). Pareto chart in Figure 11 had also revealed that bifilm index was the main factor with regard to the Fe phase length.

Dinnis [12] discussed that increasing iron concentration up to the critical iron content causes a small increase in porosity. Further increases in iron content above the critical iron content dramatically increase porosity. Gyarmati [26] used SEM to show that oxide films were detected on the inner surface of pores in RPT samples that supported the discussion that bifilms initiated porosity. Liu [27] found that beta-Fe phases were nucleating on oxides in AlCu alloys. Cao [17] proposed that increased Fe content would nucleate on oxides, and sediment them to the bottom which cleans the melt. RPT samples had shown that bifilm index was decreasing. Pore size was not changing but there was a significant decrease in the number of pores. Pores were all close to spherical. In this work, similar findings were found where the number of pores was decreasing, and their sizes were increasing (Figure 3). Other studies [13], [14] had shown that porosity was increased with increased Fe content. Khalifa [9] had reported that Fe content was more important rather than cooling rate.

## 5. Conclusions

As the holding time of the melt is increased, the bifilm index is increased which indicates decreased melt cleanliness. The increase in Fe content had no dominant effect bifilm index but the number of pores decreased, and the pore sizes increased with increased Fe content.

Bifilms tend to nucleate Fe intermetallics in A360 alloy. Regardless of the cooling rate (sand or permanent mould), the Fe phases were in the form of skeleton-type Chinese script morphology for the melts that contained higher than 180 mm bifilm index.

As the bifilm index was increased, the average length of Al-Si-Fe-Mn intermetallic was increased regardless of the cooling rate (mould type) and Fe content.

## References

- [1] Bjurenstedt, A., Ghassemali, E., Seifeddine, S. & Dahle, A.K. (2019). The effect of Fe-rich intermetallics on crack initiation in cast aluminium: An in-situ tensile study. *Materials Science and Engineering: A*. 756, 502-507. DOI:10.1016/j.msea.2018.07.044
- [2] Ferraro, S. & Timelli, G. (2015). Influence of sludge particles on the tensile properties of die-cast secondary aluminum alloys. *Metallurgical and Materials Transactions B*. 46(2), 1022-1034. DOI:10.1007/s11663-014-0260-3
- [3] Ma, Z., Samuel, A., Samuel, F., Doty, H. & Valtierra, S. (2008). A study of tensile properties in Al-Si-Cu and Al-Si-Mg alloys: Effect of  $\beta$ -iron intermetallics and porosity. *Materials Science and Engineering: A*. 490(1-2), 36-51. <https://doi.org/10.1016/j.msea.2008.01.028>
- [4] Zahedi, H., Emamy, M., Razaghian, A., Mahta, M., Campbell, J. & Tiryakioğlu, M. (2007). The effect of Fe-rich intermetallics on the Weibull distribution of tensile properties in a cast Al-5 pct Si-3 pct Cu-1 pct Fe-0.3 pct Mg alloy. *Metallurgical and Materials Transactions A*. 38(3), 659-670. DOI: 10.1007/s11661-006-9068-3
- [5] Tunçay, T., Özyürek, D., Dişpinar, D. & Tekeli, S. (2020). The effects of Cr and Zr additives on the microstructure and mechanical properties of A356 alloy. *Transactions of the Indian Institute of Metals*. 73(5), 1273-1285. DOI: 10.1007/s12666-020-01970-4
- [6] Gao, T., Hu, K., Wang, L., Zhang, B. & Liu, X. (2017). Morphological evolution and strengthening behavior of  $\alpha$ -Al (Fe, Mn) Si in Al-6Si-2Fe-xMn alloys. *Results in physics*. 7, 1051-1054. <https://doi.org/10.1016/j.rinp.2017.02.040>
- [7] Gorny, A., Manickaraj, J., Cai, Z. & Shankar, S. (2013). Evolution of Fe based intermetallic phases in Al-Si hypoeutectic casting alloys: Influence of the Si and Fe concentrations, and solidification rate. *Journal of Alloys and Compounds*. 577, 103-124. DOI: 10.1016/j.jallcom.2013.04.139
- [8] Taylor, J.A. (2012). Iron-containing intermetallic phases in Al-Si based casting alloys. *Procedia Materials Science*. 1, 19-33. <https://doi.org/10.1016/j.mspro.2012.06.004>
- [9] Khalifa, W., Samuel, F. & Gruzleski, J. (2003). Iron intermetallic phases in the Al corner of the Al-Si-Fe system. *Metallurgical and Materials Transactions A*. 34(13), 807-825. DOI:10.1007/s11661-003-1009-9
- [10] Liu, L., Mohamed, A., Samuel, A., Samuel, F., Doty, H. & Valtierra, S. (2009). Precipitation of  $\beta$ -Al<sub>5</sub>FeSi phase platelets in Al-Si based casting alloys. *Metallurgical and Materials Transactions A*. 40(10), 2457-2469. DOI:10.1007/s11661-009-9944-8
- [11] Tupaj, M., Orłowicz, A., Mróz, M., Trytek, M. & Markowska, O. (2016). Usable properties of AlSi7Mg alloy after sodium or strontium modification. *Archives of Foundry Engineering*. 16(3), 129-132. DOI:10.1515/afe-2016-0064
- [12] Dinnis, C.M., Taylor, J.A. & Dahle, A. (2006). Iron-related porosity in Al-Si-(Cu) foundry alloys. *Materials Science and Engineering: A*. 425(1-2), 286-296. DOI: 10.1016/j.msea.2006.03.045
- [13] Mikołajczak, M. & Ratke, L. (2015). Three dimensional morphology of  $\beta$ -Al<sub>5</sub>FeSi intermetallics in AlSi alloys. *Archives of Foundry Engineering*. 15(1), 47-50. DOI:10.1515/afe-2015-0010
- [14] Tunçay, T., Tekeli, S., Özyürek, D. & Dişpinar, D. (2017). Microstructure-bifilm interaction and its relation with mechanical properties in A356. *International Journal of Cast Metals Research*. 30(1), 20-29. <https://doi.org/10.1080/13640461.2016.1192826>
- [15] Cao, X. & Campbell, J. (2000). Precipitation of primary intermetallic compounds in liquid Al 11.5 Si 0.4 Mg alloy. *International Journal of Cast Metals Research*. 13(3), 175-184. <https://doi.org/10.1080/13640461.2000.11819400>
- [16] Cao, X. & Campbell, J. (2003). The nucleation of Fe-rich phases on oxide films in Al-11.5 Si-0.4 Mg cast alloys. *Metallurgical and Materials Transactions A*. 34(7), 409-1420.
- [17] Cao, X. & Campbell, J. (2004). Effect of precipitation and sedimentation of primary  $\alpha$ -Fe phase on liquid metal quality of cast Al-11.1 Si-0.4 Mg alloy. *International Journal of Cast Metals Research*. 17(1), 1-11. <https://doi.org/10.1179/136404604225014792>
- [18] Cao, X. & Campbell, J. (2004). The solidification characteristics of Fe-rich intermetallics in Al-11.5 Si-0.4 Mg cast alloys. *Metallurgical and Materials Transactions A*. 35(5), 1425-1435. DOI:10.1007/s11661-004-0251-0
- [19] Bjurenstedt, A., Casari, D., Seifeddine, S., Mathiesen, R.H. & Dahle, A.K. (2017). In-situ study of morphology and growth of primary  $\alpha$ -Al (FeMnCr) Si intermetallics in an Al-Si alloy. *Acta Materialia*. 130, 1-9.
- [20] Shabestari, S. (2004). The effect of iron and manganese on the formation of intermetallic compounds in aluminum-silicon alloys. *Materials Science and Engineering: A*. 383(2), 289-298. <https://doi.org/10.1016/j.msea.2004.06.022>
- [21] Ferraro, S., Fabrizi, A. & Timelli, G. (2015). Evolution of sludge particles in secondary die-cast aluminum alloys as function of Fe, Mn and Cr contents. *Materials Chemistry and Physics*. 153, 168-179. DOI:10.1016/j.matchemphys.2014.12.050
- [22] Dişpinar D. & Campbell, J. (2014). Reduced pressure test (RPT) for bifilm assessment. In: Tiryakioğlu, M., Campbell, J., Byszynski, G. (eds) Shape Casting: 5th International

- Symposium 2014. Springer, Cham.  
[https://doi.org/10.1007/978-3-319-48130-2\\_30](https://doi.org/10.1007/978-3-319-48130-2_30).
- [23] Gyarmati G. *et al.*, (2021). Controlled precipitation of intermetallic (Al, Si) 3Ti compound particles on double oxide films in liquid aluminum alloys. *Materials Characterization*. 181, 111467. <https://doi.org/10.1016/j.matchar.2021.111467>
- [24] Podprocká, R., Malik, J. & Bolibruchová, D. (2015). Defects in high pressure die casting process. *Manufacturing technology*. 15(4), 674-678. DOI: 10.21062/ujep/x.2015/a/1213-2489/MT/15/4/674
- [25] Samuel, A. Samuel, F. & Doty, H. (1996). Observations on the formation of  $\beta$ -Al<sub>5</sub>FeSi phase in 319 type Al-Si alloys. *Journal of Materials Science*. 31(20), 5529-5539. DOI:10.1080/13640461.2001.11819429
- [26] Gyarmati, G., Fegyverneki, G., Mende, T. & Tokár, M. (2019). Characterization of the double oxide film content of liquid aluminum alloys by computed tomography. *Materials Characterization*. 157, 109925. DOI:10.1016/j.matchar.2019.109925
- [27] Liu, K., Cao, X. & Chen, X.-G. (2011). Solidification of iron-rich intermetallic phases in Al-4.5 Cu-0.3 Fe cast alloy. *Metallurgical and Materials Transactions A*. 42(7), 2004-2016. DOI: 10.1007/s11661-010-0578-7